

**Metal-free graphitic carbon nitride nanosheet for dual mode fluorescence and  
electrochemical detection of para-nitrophenol**

Ankush Kumar Singh<sup>a§</sup>, Aayoosh Singh<sup>b§</sup>, Mithilesh Patel<sup>a</sup>, Vinod P. Singh<sup>b</sup>, Rosy<sup>a\*</sup>

<sup>a</sup>Department of Chemistry, IIT(BHU) Varanasi, India

<sup>b</sup> Department of Chemistry, Institute of Science, Banaras Hindu University, Varanasi, India

rosy.chy@iitbhu.ac.in

§Equal Contribution

**Supplementary Information**

## **2. Chemicals and Experimental Procedures**

### **2.1. Materials**

Citric acid ( $C_6H_8O_7$ ), Urea ( $NH_2CONH_2$ ), p-Nitrophenol ( $C_6H_5NO_3$ ), potassium chloride (KCl), potassium ferricyanide ( $K_3[Fe(CN)_6]$ ), Sodium dihydrogen phosphate ( $H_2NaPO_4$ ), ortho-phosphoric acid ( $H_3PO_4$ ), disodium hydrogen phosphate ( $Na_2HPO_4$ ), 2-Aminophenol, 4-Aminophenol, 2,4-Dichlorophenol (DCP), 2,4-Dinitrophenol, 2-Nitrophenol, Phenol, 2,4,6-Trichlorophenol, metal nitrate salts and anions were acquired from Alfa Aesar. The compounds were used in their original state without any further purification. A phosphate buffer solution with a concentration of 0.1 M was made following the procedure outlined by Christian and Purdy. The stock solution and test aliquots were prepared using deionized water acquired from a Milli-Q ultrapure water purifier.

### **2.2. Material Preparation**

#### **2.2.1. Synthesis of different g-CNS**

180 mg of urea mixed with 210 mg of citric acid in 30 mL distilled water and stirred for 10 minutes and then put into a 50 mL Teflon hydrothermal container, heated at  $160^\circ C$  for 180 minutes (160180) at a ramp rate of  $2^\circ$  per minute. After completion of the reaction, once the furnace reached the ambient temperature, the crucible was taken out to collect a light brown g-CNS liquid solution. Keeping all the material quantity and the ramp rate the same, we synthesized different liquid solutions of g-CNS by changing temperature and time duration, namely:  $140^\circ C$  for 90 minutes (14090),  $160^\circ C$  for 90 minutes (16090),  $160^\circ C$  for 360 minutes (160360),  $160^\circ C$  for 540 minutes (160540),  $180^\circ C$  for 90 minutes (18090),  $180^\circ C$  for 180 minutes (180180),  $180^\circ C$  for 360 minutes (180360), and  $180^\circ C$  for 540 minutes (180540).

The resultant materials were tested for the best fluorescence spectra, and  $160^\circ C$  for 180 minutes (160180) was used for further characterization.

### **2.3 Characterization details**

The crystallographic data of the synthesized material was obtained using the X-ray diffractometer (Rigaku miniflex 600, Japan), which employed a Cu-K $\alpha$  radiation source. The surface functions of g-CNS were examined using Fourier-transform infrared (FT-IR) spectroscopy. The analysis was performed using the Thermo Scientific<sup>TM</sup> Nicolet iD7 spectrometer, with a resolution of  $4\text{ cm}^{-1}$ , within the wavenumber range of  $550 - 4000\text{ cm}^{-1}$ . The ZEISS EVO scanning electron microscope was employed to get surface and morphological data. The material and modified electrode surfaces were subjected to elemental analysis using a K- $\alpha$  X-ray photon spectrophotometer produced by Thermo Fisher Scientific. The device was

fitted with a micro-focused X-ray source that employed monochromatic Al K $\alpha$  radiation, operating within an energy range of 100-4000 eV.

The structural and morphological properties of the prepared g-CNS were characterized using a Tecnai G2 20 TWIN, FEI Company of USA (S.E.A.) PTE, LTD high-resolution transmission electron microscope (HR-TEM) operated at 300 kV.

The Shimadzu UV-1800 spectrophotometer was used to take all the UV-Vis spectra. Fluorescence spectra were obtained using a Fluoromax 4CP plus fluorescence spectrophotometer (slit = 2 nm). Time-resolved fluorescence lifetime experiments (TRPL) analysis have been performed using a TCSPC system from Horiba Yovin (Delta Flex) using a picosecond diode laser (Model: delta diode).

#### *2.4. UV and Fluorescence Measurements*

g-CNS (10  $\mu$ L/mL) stock solution was prepared at room temperature in Milli-Q water for standard detection. Metal ion solutions (1 mM) were made in Milli-Q water using nitrate, chloride, or acetate salts. The tetrabutylammonium salts of respective anions (1 mM) were prepared in acetonitrile. Stock for small organic molecules 2-Aminophenol, 4-Aminophenol, 2,4-Dichlorophenol (DCP), 2,4-Dinitrophenol, 2-Nitrophenol, Phenol, and 2,4,6-trichlorophenol were prepared in Milli-Q water. The UV-vis and fluorescence spectrophotometric titrations were done directly with a microlitre pipette by adding the chemical reagents one at a time. The solution was well mixed after each aliquot was added before the spectra were taken.

#### *2.5. Electrochemical measurements*

The voltammetric analyzer designed by PalmSens3 was utilized in order to carry out the electrochemical measurements. The optimization study utilized a three-electrode setup consisting of Ag/AgCl (3M KCl) as a reference electrode, a counter electrode made of platinum wire, and a glassy carbon electrode (GCE) as a working electrode.

##### *2.5.1 Electrodeposition of g-CNS*

The glassy carbon electrode (GCE) underwent mechanical polishing using an alumina powder slurry consisting of 0.05  $\mu$ m, 0.3  $\mu$ m, and 1  $\mu$ m on a micro cloth pad prior to electrodeposition. Subsequently, the polished electrode was thoroughly rinsed using DI water. In order to do the electrodeposition of g-CNS, the aliquot utilized for electrodeposition was created by mixing different  $\mu$ L of the synthesized g-CNS liquid solution and remaining DI water to make a total solution of 1 mL with 1 mL of a 0.1M phosphate buffer of pH 7 (PB-7) in an electrochemical cell.

Cyclic voltammetry (CV) was employed for carrying out the electrodeposition of the material. To do so, the voltage was scanned from -1.0 V to +1.6 V at a scan rate of 100 mVs<sup>-1</sup>. The optimal number of scans (n) for electrodeposition was determined by systematically adjusting 'n' within the range of 5 to 25. After completing the required scans, the GCE was washed with deionized water and dried at room temperature. From this point forward, the term "g-CNS | GCE" has been used to denote the electrodeposited electrode.

### *2.5.2 Electroanalytical technique and sample preparation*

To establish the optimized number of electrodeposition cycles, the electrochemical performance of the modified electrodes with variable "n" was recorded. A comparative evaluation was conducted by measuring the square wave voltammetry (SWV) peak current of a solution containing a 1:1 ratio of 1 mM K<sub>3</sub>[Fe(CN)<sub>6</sub>] and 1 M KCl recorded using electrodes modified using different numbers of electrodeposition scans. The tests were done within a voltage range from -0.2 V to +0.6 V with a step size of 6 mV. The amplitude and frequency values were 25 mV and 10.0 Hz, respectively. After every SWV scan, the sensor was rinsed with DI water.

The electrodeposited surface's potential for voltammetric sensing applications was evaluated with p-NP as the analyte of choice. For qualitative and quantitative electroanalytical investigations, the required amount of TRP was dissolved in deionized water (DI) to make a 1 mM stock solution. The dilution method was used for preparing p-NP solutions of different concentrations. For every sample, the amount of PB-7.4 was kept fixed as 1 mL. The remaining 1 mL was composed of DI and the required volume of p-NP stock solution. The electrochemical signals were recorded using both CV (-1 V to 1 V) and SWV in a potential range of 0 to -1 V. The experimental parameters for SWV were: a step size of 6 mV and amplitude and frequency values of 25 mV and 10.0 Hz, respectively. After every SWV scan, the sensor was rinsed with DI followed by surface stabilization by recording five SWVs in a buffer solution.

### *2.6. Real Sample Preparation*

Samples of tap water, pond water and river water were collected from our lab, Agricultural Pond (IIT BHU Campus) and the Ganga River in Varanasi, respectively. The water samples were boiled for 1h and then filtered to eliminate any solid contaminants. These water samples mixed with g-CNS (10 µL/mL) for further analysis. Further samples are spiked with three different concentrations of p-NP (10, 20, and 30 µM) for fluorescence measurement and four different concentrations of p-NP (20, 30, 40, and 60 µM) for electrochemical measurements. The fluorescence spectra and electrochemical responses were recorded with the help of a

fluorescence spectrophotometer and an electrochemical workstation. The quantification table was made by recalculating the amount of p-NP using the concentration study plot.

## 2.7. Preparation of test kit for determination of p-NP

Cotton earbuds with paper stick handles were used to prepare p-NP test kits. Earbuds are made up of two parts: cotton (the sample area) and a paper stick (the holding area). A stock solution of g-CNS was prepared in Milli-Q water. Earbuds were submerged in the prepared stock solution for 10 min before drying in the air. The dried earbud test kits are now ready to detect p-NP in a pool of different analytes used.

## 2.8. Calculation of Stern-Volmer Quenching Constant

Stern–Volmer constant ( $K_{SV}$ ) calculation

The extent of fluorescence quenching was calculated using the Stern-Volmer equation:<sup>1</sup>

$$I_0/I = 1 + K_{sv}[p - NP] \quad \dots (1)$$

Where  $K_{SV}$  represents the Stern–Volmer quenching constant, and  $I_0$  and  $I$ , respectively, indicate the fluorescence intensities with or without the presence of p-NP ions at various concentrations.

## 2.9. Calculation of limit of detection (LOD)

According to the IUPAC definition, the limit of detection (LOD) for g-CNS was determined using fluorescence titration data plotted against increasing p-NP concentration. The detection limit was calculated using the following equation:<sup>2</sup>

$$LOD = \frac{3S_D}{\overline{Slope(m)}} \quad \dots (2)$$

Here, the standard deviation of blank observations is denoted by  $S_D$ , and  $m$  is the slope of intensity.

## 2.10. Fluorescence quantum yield measurements

Quantum yield g-CNS (10  $\mu$ L/mL) alone and with p-NP (1  $\mu$ M) was calculated by using the following equation:<sup>3</sup>

$$Q = Q_r \left( \frac{I}{I_r} \right) \left( \frac{OD_r}{OD} \right) \left( \frac{n_r^2}{n^2} \right) \quad \dots (3)$$

Where Q = fluorescence quantum yield, I = integrated fluorescence intensity, n = refractive index of liquid and OD = optical density (absorption). To indicate the known quantum yield of reference quinine sulphate, the subscript r is used as 0.54 in 0.1 M H<sub>2</sub>SO<sub>4</sub>.

### 2.11. Fluorescence decay measurements

Time-resolved fluorescence lifetime experiments with **g-CNS** (10 µL/mL) and **g-CNS** (10 µL/mL) with p-NP (100 µM) have been performed using a TCSPC system from Horiba Yovin (Delta Flex). Samples of **g-CNS** and **g-CNS** with p-NP were excited at 441 and 460 nm, respectively, using a picosecond diode laser (Model: delta diode). Data analysis has been performed using decay analysis software (HORIBA Scientific: EzTime).

Dynamic parameters are determined from the following equation:

$$y = A_1 * \exp\left(-\frac{x}{\tau_1}\right) + A_2 * \exp\left(-\frac{x}{\tau_2}\right) + y_0 \quad \dots$$

(4)

Weighted mean lifetime  $\langle \tau \rangle$  was calculated by using the following equation:

$$\langle \tau \rangle = (A_1 \tau_1 + A_2 \tau_2) / (A_1 + A_2) \quad \dots \quad (5)$$

Where  $A_1/A_2$  and  $\tau_1/\tau_2$  are the fractions or amplitudes (A) and lifetimes ( $\tau$ ), respectively.

The radiative rate constant ( $K_r$ ) and non-radiative rate constant ( $K_{nr}$ ) are calculated from the following equations:<sup>4</sup>

$$\langle \tau^{-1} \rangle = (K_r + K_{nr}) \quad \dots$$

(6)

$$K_r = \frac{\Phi}{\langle \tau \rangle} \quad \dots$$

(7)

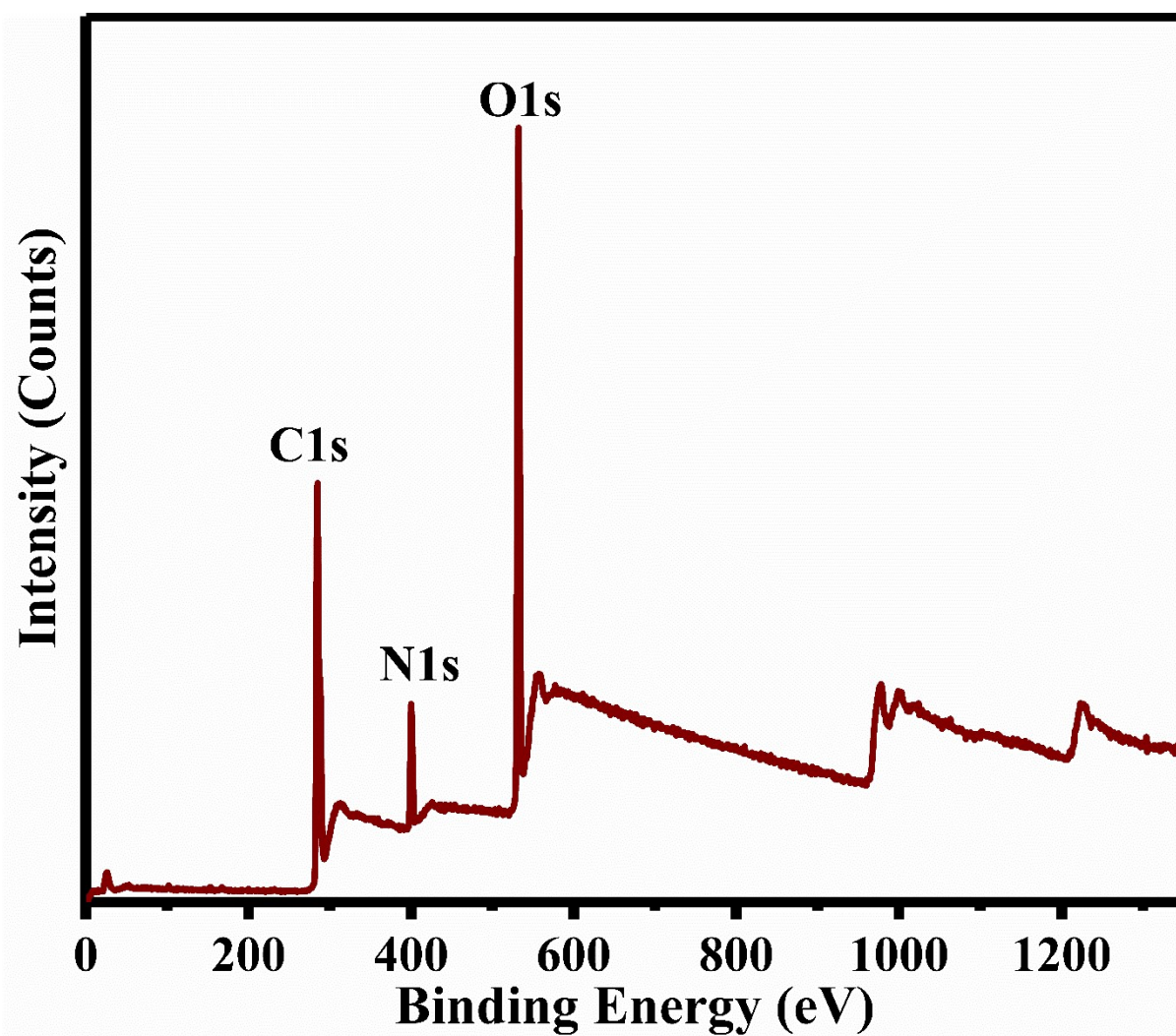
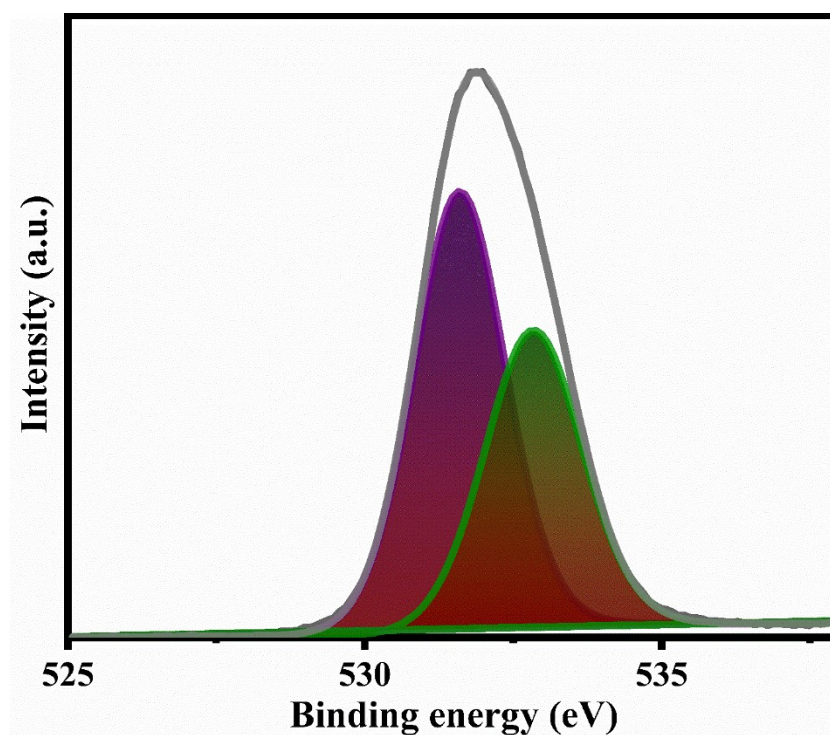
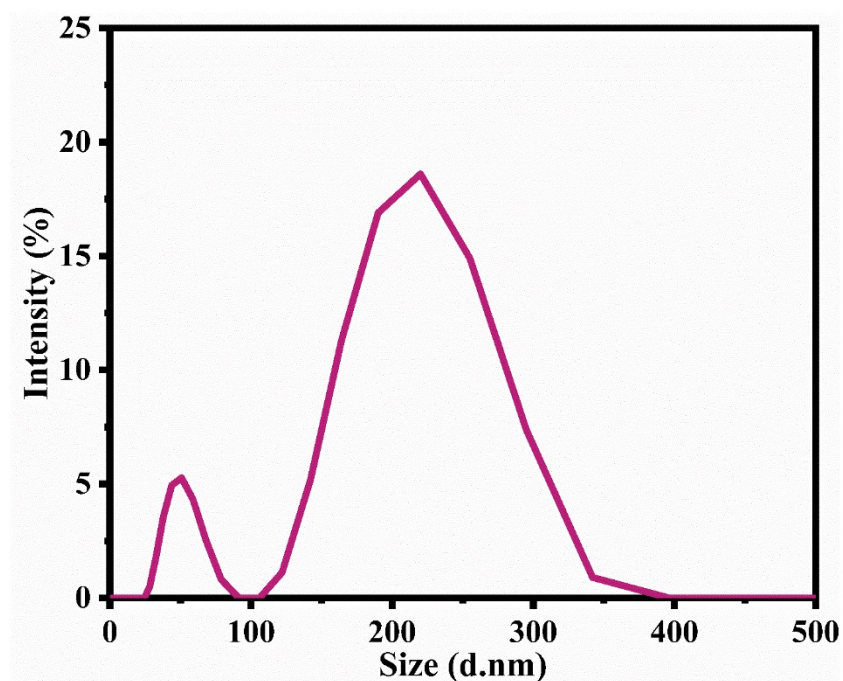


Figure SI-1: Full survey spectra of synthesized g-CNS



**Figure SI-2:** O 1s spectra of synthesized g-CNS



**Figure SI-3:** DLS spectrum of as-synthesized g-CNS.



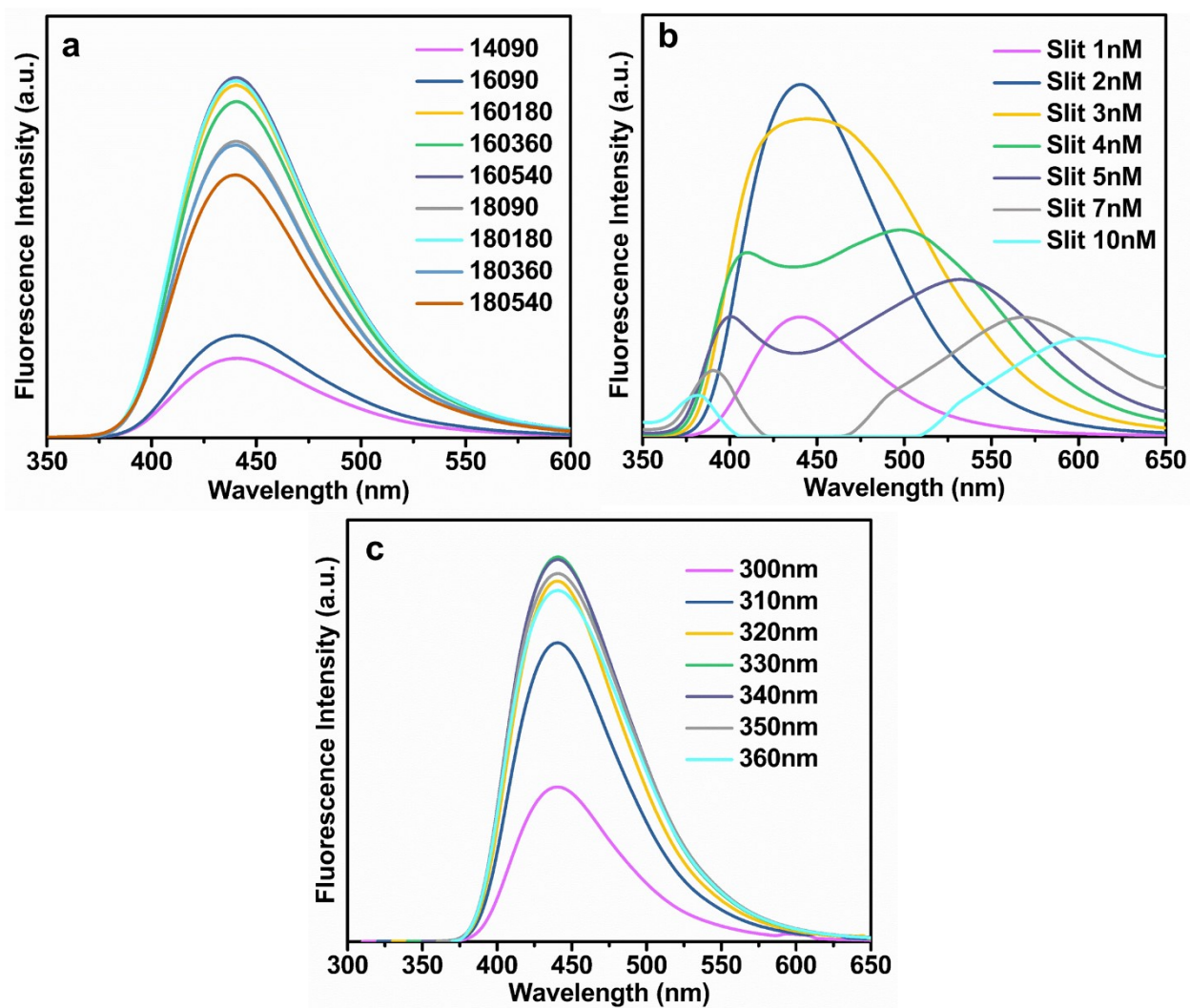


**Figure SI-4:** (a) Fluorescence intensity response of different synthesized g-CNS; (b) Fluorescence intensity responses of the best g-CNS at different slit widths; (c) Fluorescence intensity responses of the best g-CNS (2 nM) at different excitation wavelengths.



**Figure SI-5:** Photograph clicked for the 10  $\mu\text{L/mL}$  g-CNS solution in visible light and UV light.

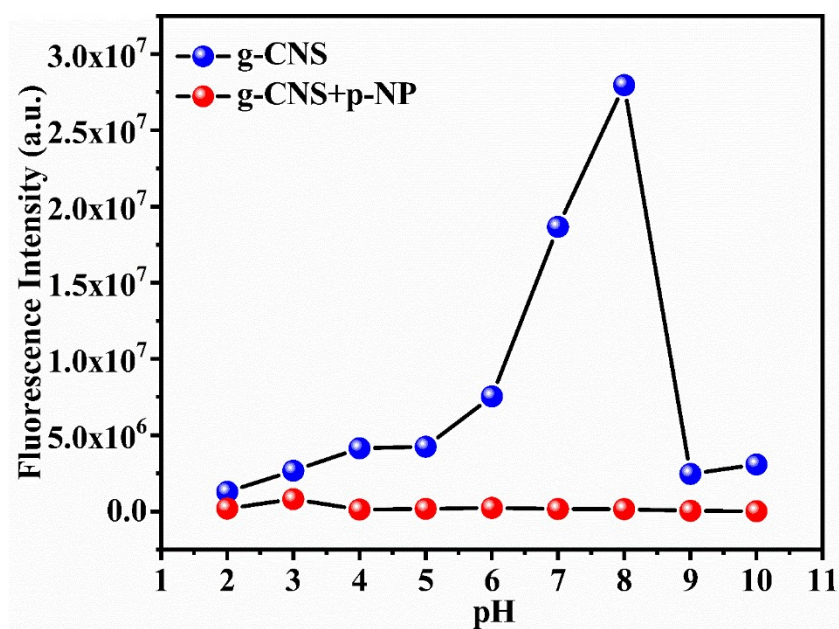


**Figure SI-6:** Fluorescence intensity of as-synthesized g-CNS and g-CNS with 1 mM of p-NP for different pH.

**Table SI-1.** Comparison of the reported fluorescence sensors developed for p-NP estimation using quantum dots, metal oxides, and similar surface modifications with the proposed g-CNS probe.

Probe	Linear range ( $\mu\text{M}$ )	LOD ( $\mu\text{M}$ )	Reference
CDs@PDA	2–34	3.44	5
GSH-Au/Ag NCs@ZIF-8	2–35	1.1	6
B,N-CDs	0.5-60	0.2	7
N-doped oxidized carbon dots	2–100	1.2	8
Si NPs	0.5-60	0.074	9
N, S-CQDs	0.05-125	0.039	10
Cadmium(II)-MOF	0–30	6.84	11
Cyclodextrin-Au nanocluster	0.1-100	0.09	12
Cu-CDs	0.5–50	0.08	13
g-CNS	1-100	0.036	<b>Present work</b>

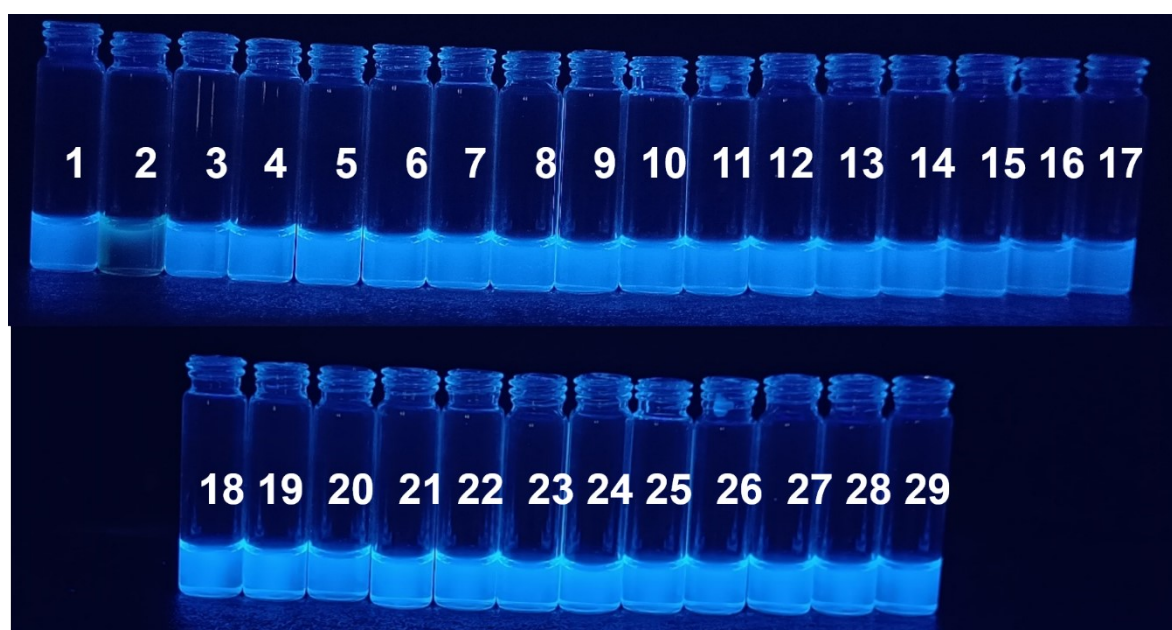


**Figure SI-7:** Photograph taken under UV light for (1) g-CNS and g-CNS + other analytes like (2) p-NP, (3)  $\text{Al}^{3+}$ , (4)  $\text{Co}^{2+}$ , (5)  $\text{Cr}^{3+}$ , (6)  $\text{Cu}^{2+}$ , (7)  $\text{Fe}^{3+}$ , (8)  $\text{Hg}^{2+}$ , (9)  $\text{Na}^+$ , (10)  $\text{K}^+$ , (11)  $\text{Mn}^{2+}$ , (12)  $\text{Ni}^{2+}$ , (13)  $\text{Pb}^{2+}$ , (14)  $\text{Zn}^{2+}$ , (15)  $\text{F}^-$ , (16)  $\text{Cl}^-$ , (17)  $\text{I}^-$ , (18)  $\text{OH}^-$ , (19)  $\text{SO}_4^{2-}$ , (20)  $\text{HSO}_4^-$ , (21)  $\text{CO}_3^{2-}$ , (22)  $\text{CH}_3\text{COO}^-$ , (23)  $\text{CN}^-$ , (24) 2-Aminophenol, (25) 4-Aminophenol, (26) 2,4 Dichlorophenol (DCP), (27) 2,4-Dinitrophenol, (28) 2-Nitrophenol, and (29) Phenol.

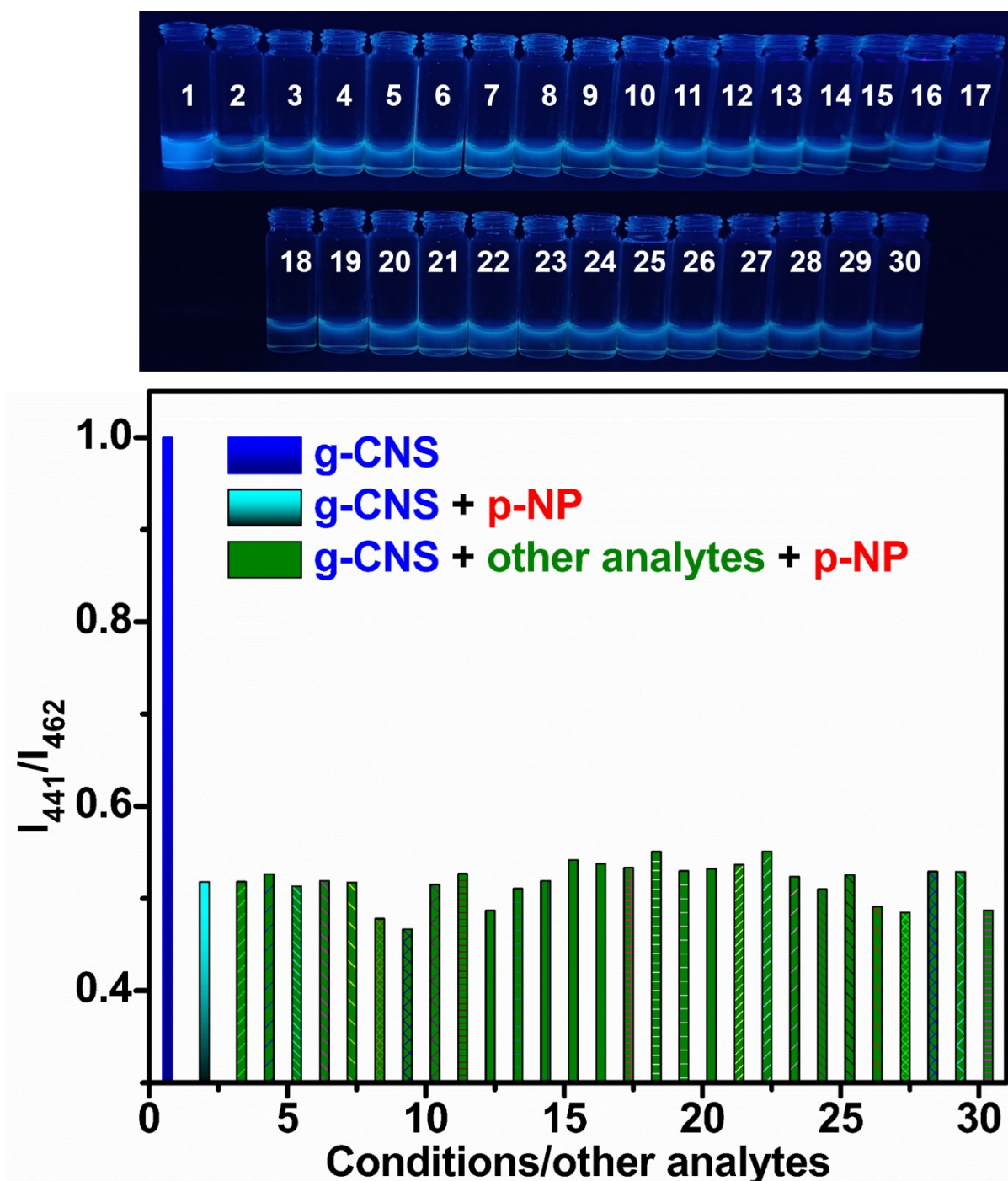


**Figure SI-8:** (above) photograph taken under UV light; (below) bar diagram of the competitive experiments of different analytes, (1) g-CNS probe, (2) g-CNS + 100  $\mu$ M p-NP, g-CNS + p-NP + (3)  $\text{Al}^{3+}$ , (4)  $\text{Co}^{2+}$ , (5)  $\text{Cr}^{3+}$ , (6)  $\text{Cu}^{2+}$ , (7)  $\text{Fe}^{3+}$ , (8)  $\text{Hg}^{2+}$ , (9)  $\text{Na}^+$ , (10)  $\text{K}^+$ , (11)  $\text{Mn}^{2+}$ , (12)  $\text{Ni}^{2+}$ , (13)  $\text{Pb}^{2+}$ , (14)  $\text{Zn}^{2+}$ , (15)  $\text{F}^-$ , (16)  $\text{Cl}^-$ , (17)  $\text{I}^-$ , (18)  $\text{OH}^-$ , (19)  $\text{SO}_4^{2-}$ , (20)  $\text{HSO}_4^-$ , (21)  $\text{CO}_3^{2-}$ , (22)  $\text{CH}_3\text{COO}^-$ , (23)  $\text{CN}^-$ , (24) 2-Aminophenol, (25) 4-Aminophenol, (26) 2,4-Dichlorophenol (DCP), (27) 2,4-Dinitrophenol, (28) 2-Nitrophenol, (29) Phenol, and (30) 2,4,6-Trichlorophenol.



**Table SI-2.** Quantum yields and fluorescence decay parameters of **g-CNS** (10  $\mu\text{L/ml}$ ) alone and after treatment with p-NP (100  $\mu\text{M}$ ).

Sample	A (%)	$\tau$ (ns)	$\langle\tau\rangle$ (ns)	$\Phi_f(10^{-3})$	$K_r(\cdot s)(10^6)$	$K_{nr}(\cdot s)(10^9)$
<b>g-CNS</b>	99.99 ( $A_1$ ) 0.01 ( $A_2$ )	0.049 ( $\tau_1$ ) 0.183 ( $\tau_2$ )	0.049	1.69	34.42	2.03
<b>g-CNS+PNP</b>	99.02 ( $A_1$ ) 0.98 ( $A_2$ )	0.048 ( $\tau_1$ ) 0.135 ( $\tau_2$ )	0.048	0.40	8.35	2.08

**Table SI-3** Detection of p-NP in real water samples using the fluorescence method.

Sample	Added p-NP ( $\mu\text{M}$ )	Detected p-NP ( $\mu\text{M}$ )	Recovery (%)
<b>Tap water</b>	10	9.80	98.00
	20	19.55	97.75
	30	29.07	96.90
<b>Pond water</b>	10	9.87	98.70
	20	19.56	97.80
	30	29.06	96.86
<b>Ganga river</b>	10	9.62	96.20
	20	19.15	95.75
	30	28.61	95.36

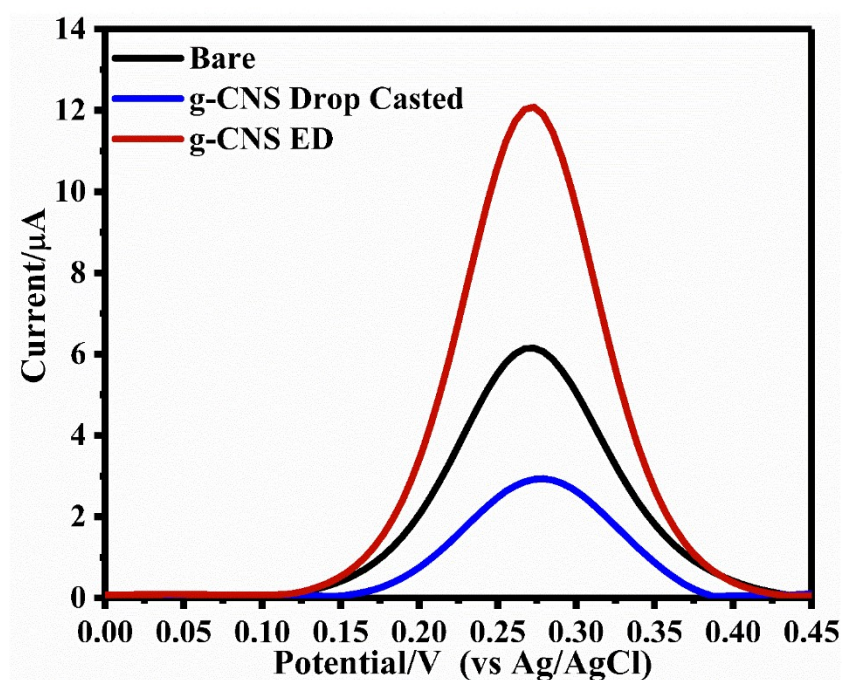


**Figure SI-9:** Comparison study of bare GCE, drop-cast GCE and electrodeposited GCE in 1 mM  $\text{K}_3[\text{Fe}(\text{CN})_6]$  solution in 1M KCl solution.

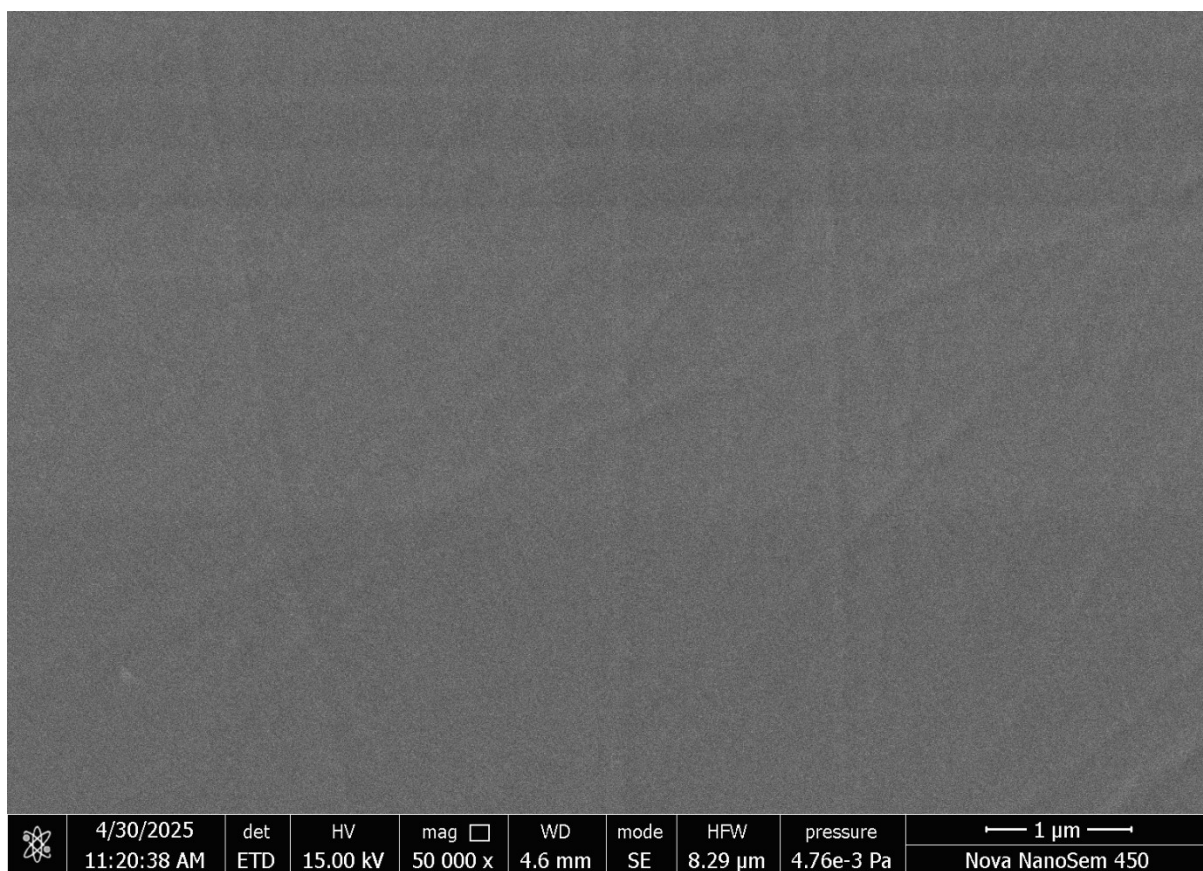


**Figure SI-10:** HR-SEM image of uncoated GCE.

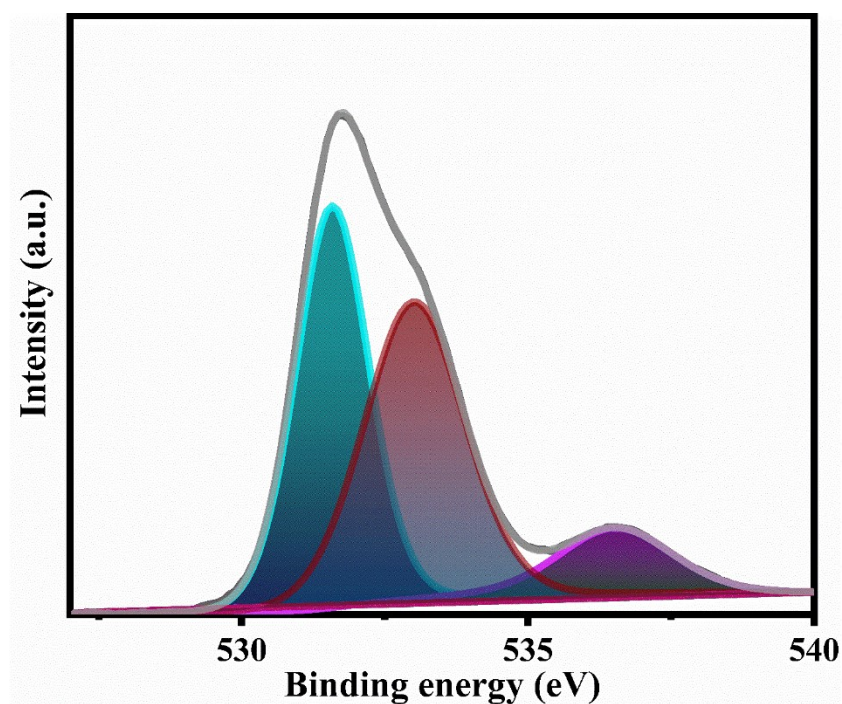


**Figure SI-11:** O 1s spectra of electrodeposited g-CNS interface.

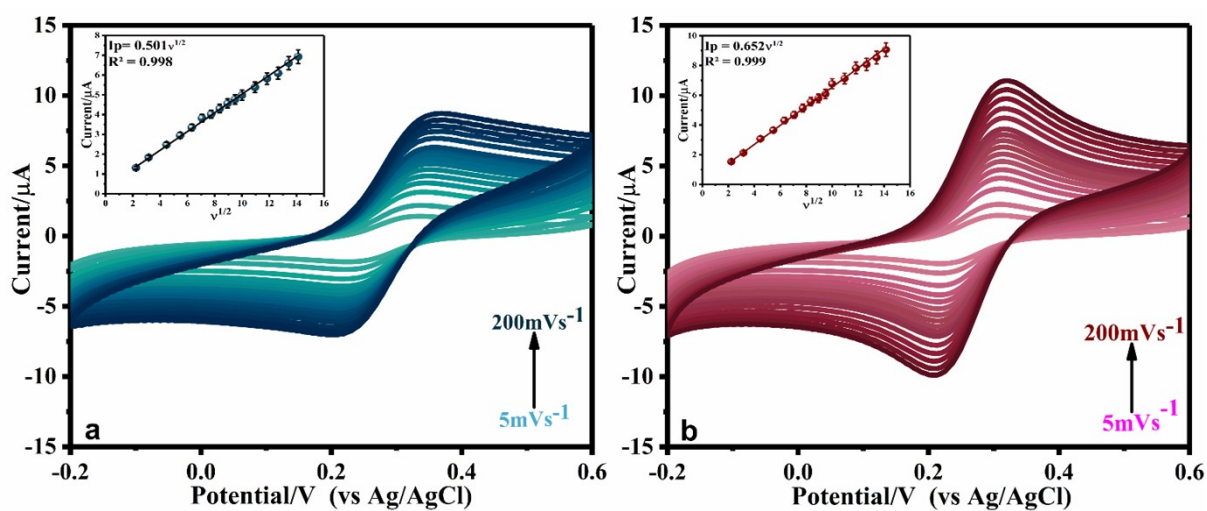


**Figure SI-12:** Scan Rate study and linear regression plot between  $I_p$  vs  $v^{1/2}$  (a) Bare GCE (b) g-CNS Coated GCE.

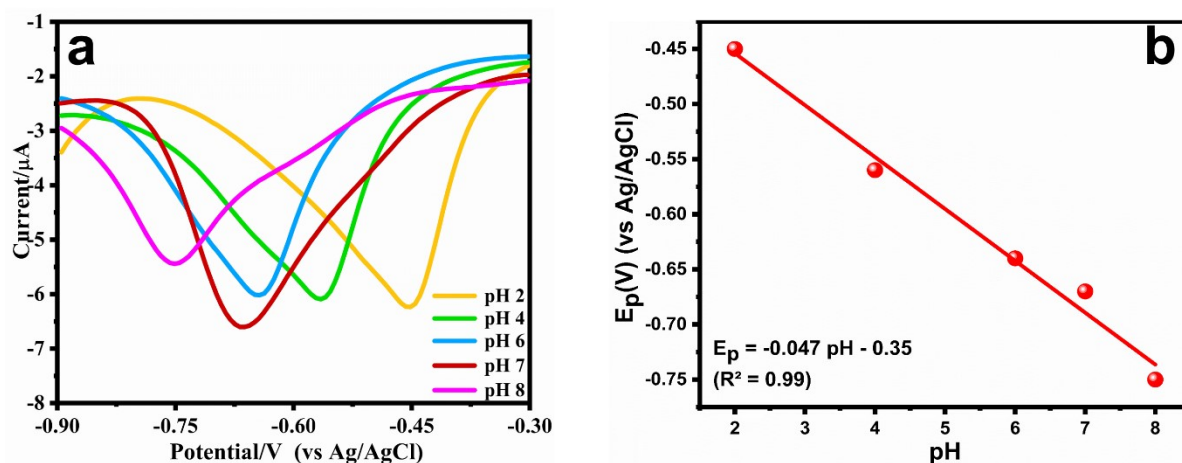


**Figure SI-13:** (a) SWV response of 45  $\mu\text{M}$  of p-NP at different pH for the coated interface. (b) Linear plot obtained from peak potential as a function of pH.

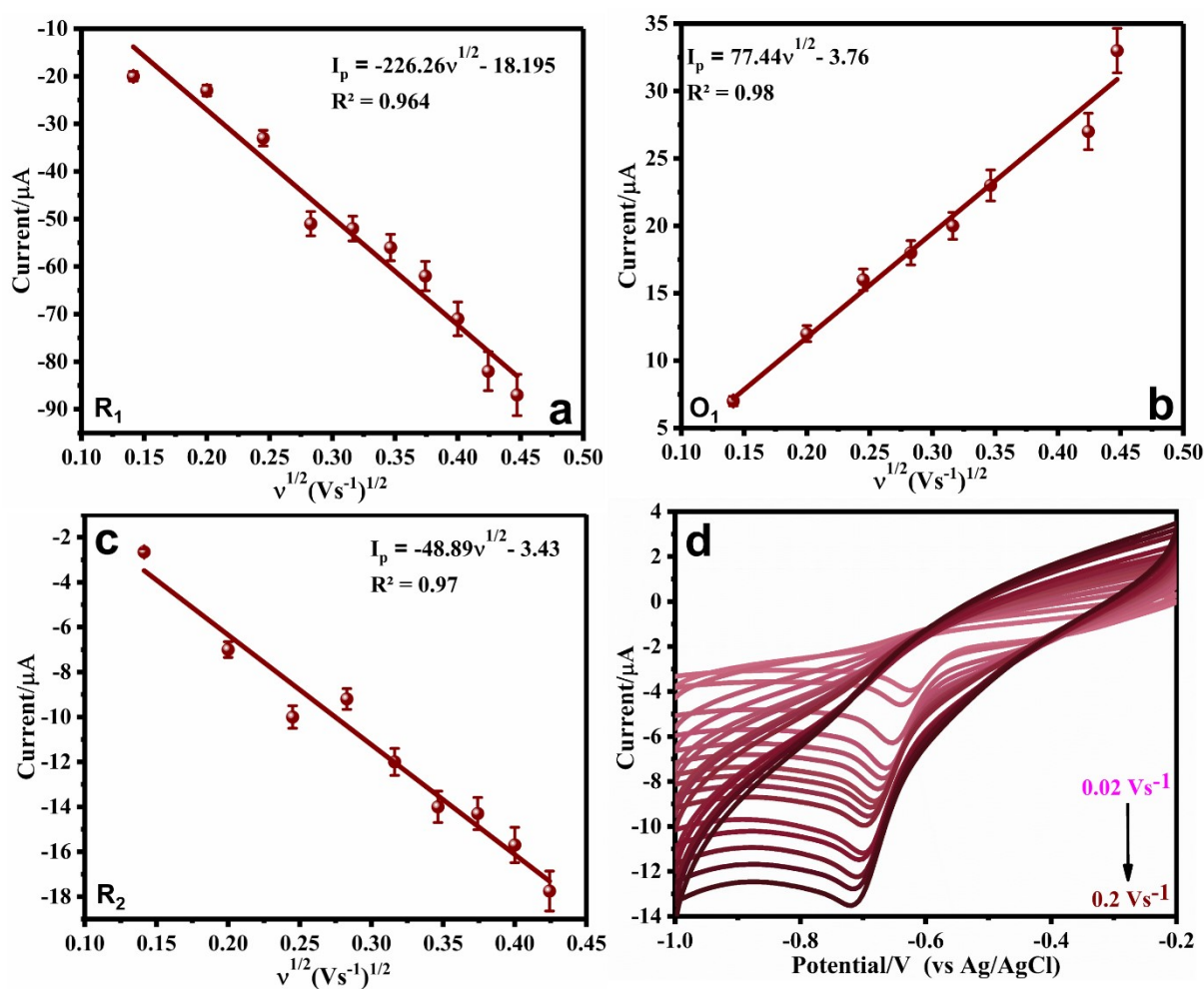


**Figure SI-14:** Plot of  $I_p$  Vs  $v^{1/2}$  for different scan rates on g-CNS | GCE interface for 100  $\mu\text{M}$  p-NP utilizing (a)  $R_1$  CV peaks, (b)  $O_1$  CV peaks and (c)  $R_2$  CV peaks; Scan rate study of 100  $\mu\text{M}$  p-NP in the range of  $R_1$  CV peaks.



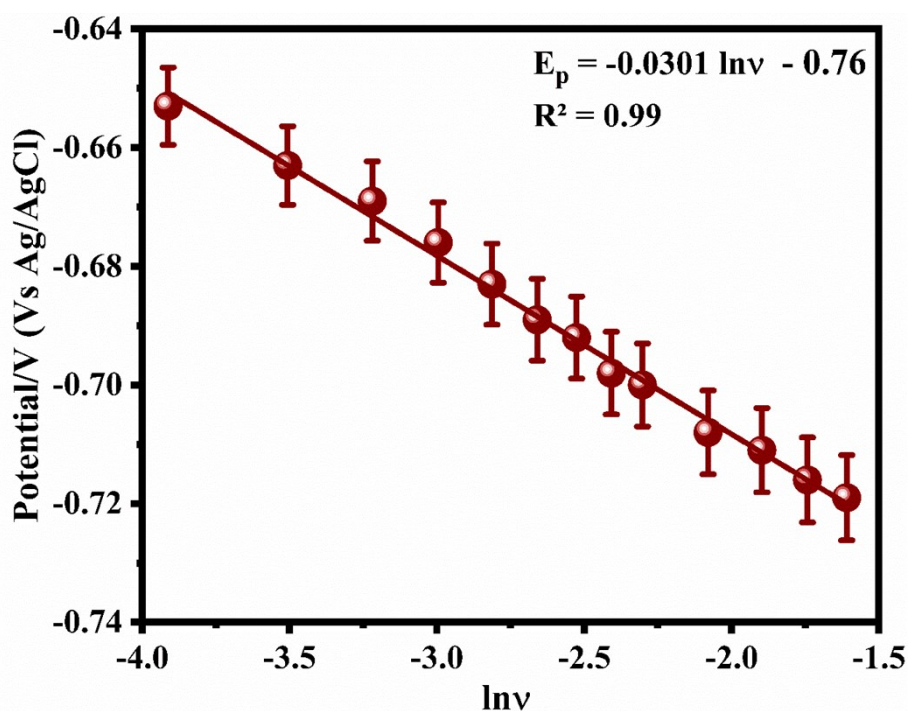


**Figure SI-15:** Plot between  $E_p$  vs  $\ln v$  for the calculation of the number of electron transfers for the reduction peak ( $R_1$ ) for p-NP.

**Table SI-4:** Comparison of the reported electrochemical sensors developed for p-NP estimation using gCN, metal oxides, and similar surface modifications with the proposed gCN.MnO<sub>2</sub>/SPE scaffold.

Modified Interface	Linear range( $\mu$ M)	LOD( $\mu$ M)	Technique	Reference
PRB/PGE	5–700	1.78	DPV	13
f-MWCNTs	0.001–2190	0.32	LSV	14
PDPP–GO/GCE	0.5–163	0.10	DPV	15
SnO <sub>2</sub> /ZIF-8/g-C <sub>3</sub> N <sub>4</sub> /GC	10–100	0.565	DVP	16
(CeGdHfPrZr)O <sub>2</sub> /GCE	5–100	0.32	SWV	17
g-C <sub>3</sub> N <sub>4</sub> /V <sub>2</sub> O <sub>5</sub> /GCE	0.001–100	0.85	SWV	18
Au-rGO/AC/GCE	72–4400	1.12	LSV	19
rGO-MoS <sub>2</sub> /Fe <sub>3</sub> O <sub>4</sub>	10–400	0.8	DPV	20
NCC/GCE	1–20	2.48	CV	21
Graphene-Nafion/SPE	10–900	0.6	DPV	22
OMCs/GCE	2.0–90	0.1	DPV	23
g-CNS   GCE	5-100	0.218	SWV	<b>Present work</b>

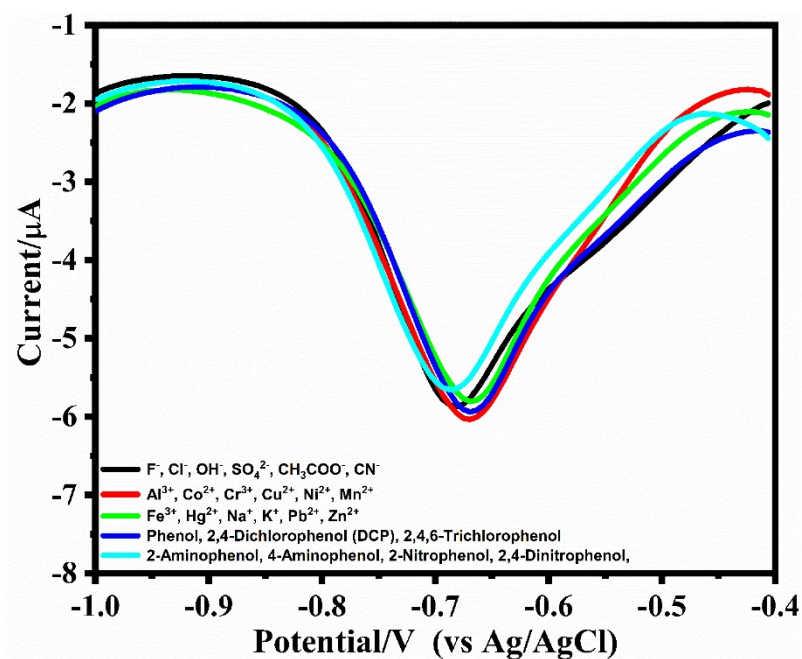


**Figure SI- 16:** Interference Study of g-CNS | GCE for 45  $\mu\text{M}$  of p-NP with same concentration of ;(Black)  $\text{F}^-$ ,  $\text{Cl}^-$ ,  $\text{OH}^-$ ,  $\text{SO}_4^{2-}$ ,  $\text{CH}_3\text{COO}^-$  and  $\text{CN}^-$ ; (Red)  $\text{Al}^{3+}$ ,  $\text{Co}^{2+}$ ,  $\text{Cr}^{3+}$ ,  $\text{Cu}^{2+}$ ,  $\text{Ni}^{2+}$ , and  $\text{Mn}^{2+}$ ; (Green)  $\text{Fe}^{3+}$ ,  $\text{Hg}^{2+}$ ,  $\text{Na}^+$ ,  $\text{K}^+$ ,  $\text{Pb}^{2+}$  and  $\text{Zn}^{2+}$ , (Blue) Phenol, 2,4-Dichlorophenol (DCP), 2,4,6-Trichlorophenol; (Cyan) 2-Aminophenol, 4-Aminophenol, 2-Nitrophenol, and 2,4-Dinitrophenol.

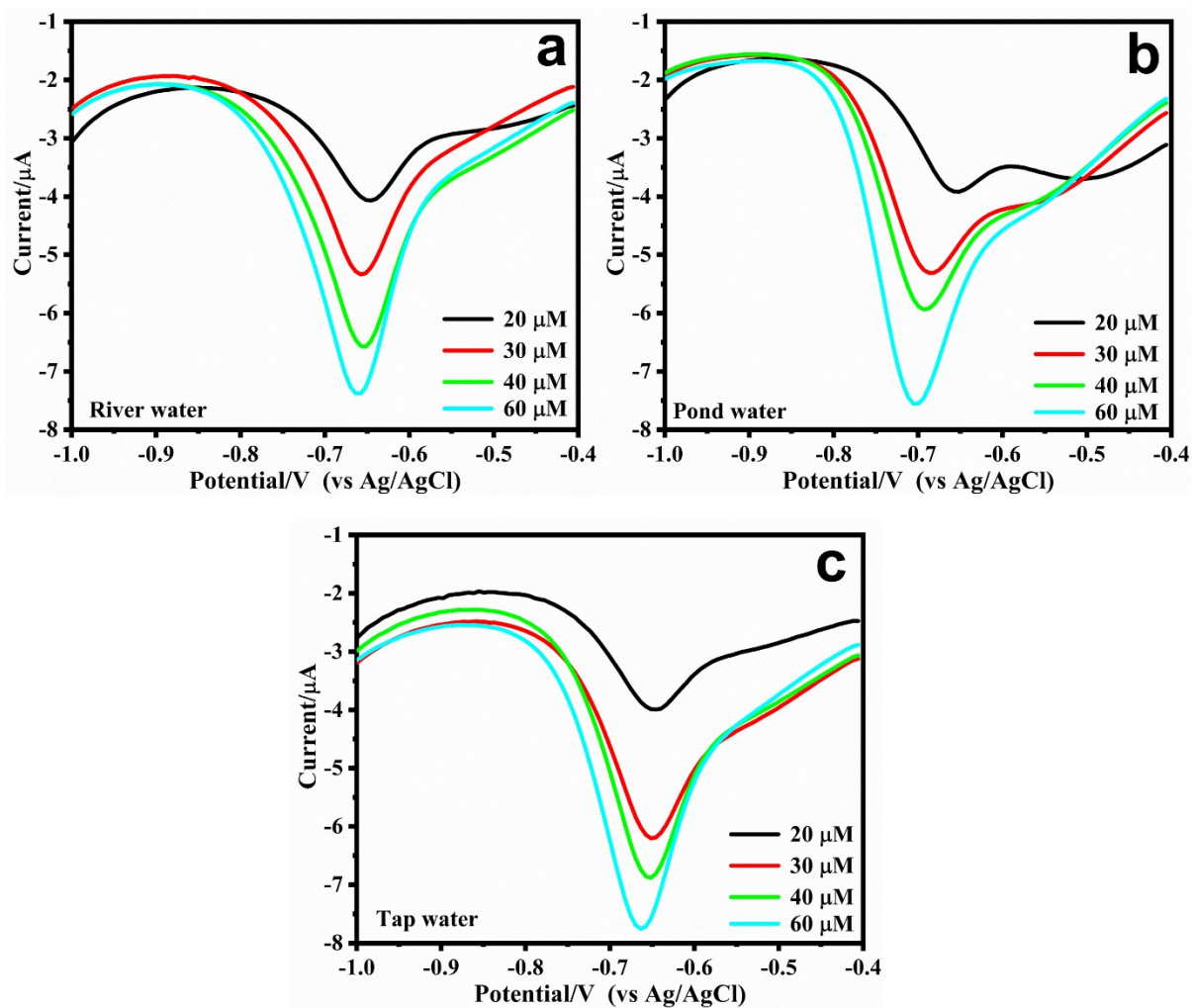


**Figure SI-17:** Real sample analysis on coated interface for different spiked concentrations of p-NP; (a) Ganga River water (b) pond water (c) tap water.

**Table SI-5:** Quantification of p-NP in real samples using g-CNS | GCE

Sample	Current ( $\mu\text{A}$ )	Detected ( $\mu\text{M}$ )	Actual ( $\mu\text{M}$ )	Error (%)
<b>River water</b>				
1	-1.71	20.62	20	3.10
2	-3.20	30.00	30	0.00
3	-4.10	41.07	40	2.69
4	-5.03	56.70	60	5.49
<b>Pond water</b>				
1	-1.53	19.49	20	2.54
2	-3.19	29.93	30	0.20
3	-3.91	38.55	40	3.61
4	-5.50	64.94	60	8.23
<b>Tap Water</b>				
1	2.54	20.75	20	3.77
2	0.20	28.47	30	5.07
3	3.61	41.35	40	3.38
4	8.23	55.35	60	7.74

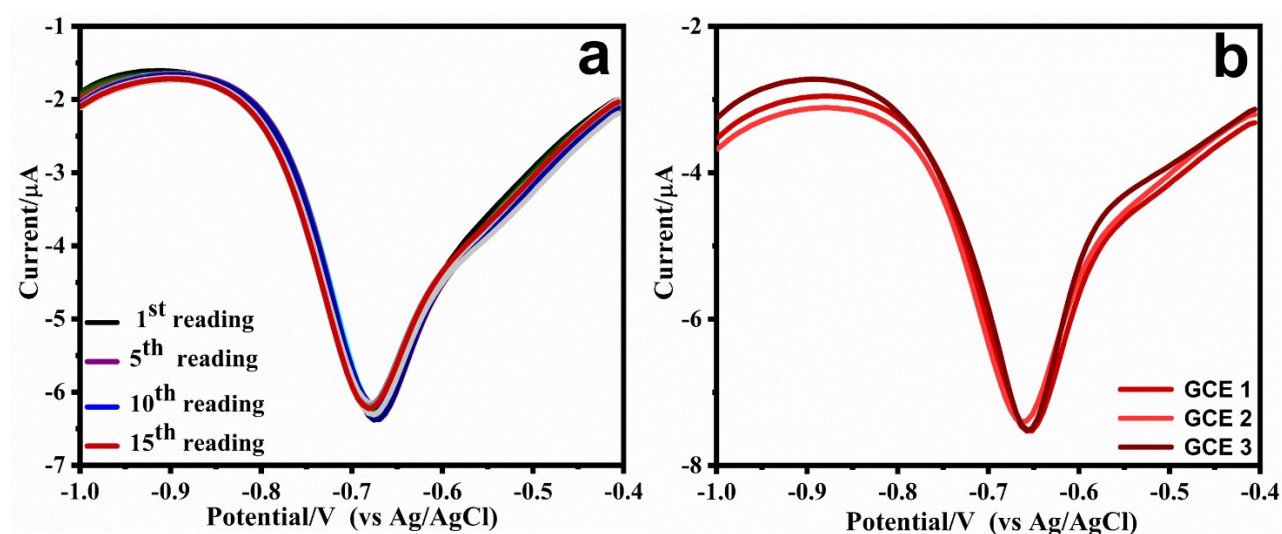


**Figure SI-18:** (a) Repetitive SWV current response of g-CNS | GCE in 45  $\mu\text{M}$  of p-NP. (b) Reproducibility study at different GCE after modification with g-CNS in 45  $\mu\text{M}$  of p-NP.

## References

- 1 M. H. Gehlen, *J. Photochem. Photobiol. C Photochem. Rev.*, 2020, **42**, 100338.
- 2 G. L. Long and J. D. Winefordner, *Am. Chem. Soc.*, 1983, **55**, 712A–724A.
- 3 P. Yadav, A. Singh, G. Kumar, S. Singh and V. P. Singh, *Spectrochim. Acta Part A Mol. Biomol. Spectrosc.*, 2025, **329**, 125557.
- 4 A. Singh, P. Yadav, S. Singh, P. Kumar, S. Srikrishna and V. P. Singh, *J. Mater.*

- Chem. C*, 2023, **11**, 13056–13066.
- 5 Q. Liu, F. Zhao, B. Shi and L. Changli, *Luminescence*, 2021, **36**, 431–442.
  - 6 T. Zhou, L. Zang, J. Sun, X. Zhang, Z. Qu, X. Liu, G. Zhang, X. Wang, F. Wang and Z. Zhang, *Colloids Surfaces A Physicochem. Eng. Asp.*, 2025, **708**, 135999. (<https://doi.org/10.1016/j.colsurfa.2024.135999>)
  - 7 N. Xiao, S. G. Liu, S. Mo, N. Li, Y. J. Ju, Y. Ling, N. B. Li and H. Q. Luo, *Talanta*, 2018, **184**, 184–192 (<https://doi.org/10.1016/j.talanta.2018.02.114>).
  - 8 N. K. R. Bogireddy, R. Cruz Silva, M. A. Valenzuela and V. Agarwal, *J. Hazard. Mater.*, 2020, **386**, 121643.
  - 9 F. Liu, F. Liang, Z. Li, G. Kang, T. Wang, C. Chen and Y. Lu, *Analyst*, 2023, **148**, 4030–4036.
  - 10 Q. Zhang, H. Mei, W. Zhou and X. Wang, *Microchem. J.*, 2021, **162**, 105842.
  - 11 E. Kavak, M. Şevik and M. Arici, *J. Photochem. Photobiol. A Chem.*, 2023, **445**, 115032.
  - 12 Y. Li, Q. L. Wen, A. Y. Liu, Y. Long, P. Liu, J. Ling, Z. T. Ding and Q. E. Cao, *Microchim. Acta*, 2020, **187**, 1–9.
  - 13 J. Fang, S. Zhuo and C. Zhu, *Opt. Mater. (Amst.)*, 2019, **97**, 109396.
  - 14 R. Nehru, T. W. Chen, S. M. Chen, T. W. Tseng and X. Liu, *Int. J. Electrochem. Sci.*, 2018, **13**, 7778–7788.
  - 15 L. Jia, J. Hao, S. Wang, L. Yang and K. Liu, *RSC Adv.*, 2023, **13**, 2392–2401.
  - 16 D. Mohanta, A. Mahanta, S. R. Mishra, S. Jasimuddin and M. Ahmaruzzaman, *Environ. Res.*, 2021, **197**, 111077.
  - 17 M. Anandkumar, P. K. Kannan, R. S. Morozov, O. V. Zaitseva, S. Sudarsan and E. A. Trofimov, *Ceram. Int.*, 2025, **51**, 2770–2778.
  - 18 D. Sangamithirai and S. Ramanathan, *Electrochim. Acta*, 2022, **434**, 141308.
  - 19 F. A. Harraz, M. A. Rashed, M. Faisal, M. Alsaiari and S. A. Alsareii, *Colloids Surfaces A Physicochem. Eng. Asp.*, 2022, **654**, 130068.
  - 20 S. Kalia, R. Kumar, R. Sharma, S. Kumar, D. Singh and R. K. Singh, *J. Phys. Chem. Solids*, 2024, **184**, 111719.
  - 21 N. Ahmad, M. Alam, R. Wahab, J. Ahmad, M. Ubaidullah, A. A. Ansari and N. M. Alotaibi, *J. Mater. Sci. Mater. Electron.*, 2019, **30**, 17643–17653.
  - 22 A. Arvinte, M. Mahosenaho, M. Pinteala, A. M. Sesay and V. Virtanen, *Microchim. Acta*, 2011, **174**, 337–343.
  - 23 T. Zhang, Q. Lang, D. Yang, L. Li, L. Zeng, C. Zheng, T. Li, M. Wei and A. Liu, *Electrochim. Acta*, 2013, **106**, 127–134.